RESEARCH ARTICLE

In-silico and *In-vitro* Studies on Targeting Tumor Apoptosis by Activating Caspase-3

Akula Sowjanya[1*], G. Shiva Kumar[2]

[1]*Department of Pharmacology, GITAM School of Pharmacy (GITAM Deemed to be University), Rudraram, Hyderabad, Telangana, India.*

[2]*GITAM School of Pharmacy (GITAM Deemed to be University), Rudraram, Hyderabad, Telangana, India*

Received: 13th February, 2023; Revised: 22nd June, 2023; Accepted: 13th August, 2023; Available Online: 25th September, 2023

ABSTRACT

Background: Despite the availability of numerous treatment options, cancer remains the primary cause of death in the current decade. The present study integrates computational and experimental methods to identify and develop a novel promising compound with anticancer properties. The study aims to evaluate the potential anticancer properties of selected molecules based on docking score, compliance with Lipinski's rule of five, and *in-silico* safety prediction. Structure drug design by molecular docking methods was used to explore ligand conformations at various target binding sites. The *in-silico* physicochemical, pharmacokinetic, and toxicology properties of designed molecules were predicted using online software. Further, *in-vitro*, anticancer properties were studied by MTT Assay and flow cytometry.

Results: 2-Butyl-3- (3, 5-diiodo-4- hydroxybenzoyl) benzofuran is one of the selected ligands showed potent anticancer activity against HT- 29 (Human Colon Cancer) cells and A549 (Human lung cancer) at IC50 concentrations. Further apoptosis studies demonstrated the possible mode of action against HT-29 cells. The proposed mechanism of action may be caspase-3 activation. As a consequence of caspase-3 activation, enzymes such as DNase are activated, leading to DNA fragmentation and apoptosis, and DNA fragmentation was 6.5 times greater than in untreated cells. The IC_{50} concentration of 2-Butyl-3- (3, 5-diiodo-4- hydroxybenzoyl) benzofuran inhibited 50% of HT-29 cells during G0/G1 phase.

Conclusion: This research contributes to the burgeoning field of integrated *in-vitro* and *in-silico* analysis of biological systems, which can be used to study complicated cancer cell population dynamics. Future studies should investigate the impact on Human lung cancer cells.

Keywords: BCL-2 assay, Cell cycle analysis, caspase-3 activity, *In-silico* study, MTT assay, Tunel assay.

International Journal of Pharmaceutical Quality Assurance (2023); DOI: 10.25258/ijpqa.14.3.34

How to cite this article: Sowjanya A, Kumar GS. *In-silico* and *In-vitro* Studies on Targeting Tumor Apoptosis by Activating Caspase-3. International Journal of Pharmaceutical Quality Assurance. 2023;14(3):661-670.

Source of support: Nil.

Conflict of interest: None

INTRODUCTION

One in every six deaths globally is caused by cancer. Nearly 10 million cancer deaths were reported in 2020. The most prevalent cancers include prostate cancer (1.41 million cases), lung cancer (2.21 million cases), colon and rectum cancers (1.93 million cases), and breast cancer (2.26 million cases). Hepatitis and human papillomaviruses (HPVs) are responsible for about 30% of cancer cases in low- and lower-middle-income nations. Numerous malignancies may be cured through early detection and effective treatment. Due to the asymptomatic character of lung cancer, it is typically diagnosed at an advanced stage.[1,2] Even though some chemotherapeutic agents have relatively favorable effects on certain types of cancer, a chemotherapeutic agent that can effectively cure lung cancer has not yet been discovered. Breast cancer is the leading cause of cancer-related fatalities among women. Radiation therapy and chemotherapy are the most effective forms of defense, but their side effects on healthy cells and drug resistance make them inadequate.[3]

Numerous studies are investigating novel compounds for the treatment of cancer. Despite the failure of innumerable treatments thus far due to intolerance and resistance, the progression of the disease persists.[4,5] At the end of the literature review, all selected ligands are novel and not reported for any research activity. In the initial phase of this study, human carcinoma cell lines A549 (lung cancer), MCF-7 (human breast cancer), HT-29 (human colon cancer), and DU145 (human prostate cancer) were used to assess the anticancer effects of samples 1, 2, 3, 4, 5, 6, 7, and 8. In addition, we plan to evaluate the pharmacological effects of promising molecules on HT-29 cells in the preliminary screening.

**Author for Correspondence: akula.sowjuu@gmail.com*

MATERIALS AND METHODS

In-silico Methods

Structure-based drug design and molecular docking studies

Ligand docking studies were performed by Molegro Virtual Docker (Molegro A.P.S., Aarhus C. Denmark). MVD is the fast and flexible docking program that gives the most likely ligand binding conformation to a macromolecule.[6] More than a hundred compounds were selected in search of new ligands for the Tubulin protein- PDB: 1SA0, Anaplastic lymphoma kinase (ALK)-PDB:6MX8, Estrogen Receptor (ER)- PDB:3ERT and Epidermal Growth Factor Receptor(EGFR)-PDB:1M17 as an anticancer drug like candidate. The 3D structures of drugs and other chemical structures were downloaded from the PubChem chemical database and drug bank, drawn using the Chem Draw software, and saved in the mol format after energy minimization.[7,8]

Target proteins were downloaded as pdb files from the protein data bank for docking studies. The PDB files contain insufficient or absent assignments of explicit hydrogens, and the PDB file format cannot store bond order information. Consequently, proper bonds, bond orders, hybridization, and charges were designated to the protein during its preparation with the MVD. The workspace is populated with the selected protein chain without co-crystallized ligands and water molecules. MVD's built-in cavity detection algorithm was utilized to compute the potential binding sites of the targets after the surface was generated. Ligands are imported into the workstation and subsequently prepared. The grid was developed around the co-crystallized ligand's binding pocket, and docking was performed after setting other parameters. The moldock score of ligands is contrasted to that of standard drugs.

In-silico pharmacokinetic (ADME) properties

Swiss ADME online software was used to forecast the physicochemical properties of designed molecules. The Molecular Modelling Group of the Swiss Institute of Bioinformatics develops and maintains it: http://www.swissadme.ch/index.php.[9] It uses open Babel's definition for descriptors such as atom/bond/group counts and molecular refractivity. This website enables the computation of physicochemical descriptors and the prediction of the pharmacokinetic properties and drug-like nature of a single or multiple small, neutral molecules with aromatic or kekule descriptions.[10]

In-silico toxicity risk assessment

The safety of the designed compounds was predicted by Data Warrior (version v04.04.04) developed at actelion Pharmaceuticals Ltd. http://www.openmolecules.org/datawarrior/. It is a free chem informatics program for data visualization and analysis. Data Warrior can compute several physicochemical characteristics, factors relating to lead-likeness or drug-likeness, ligand efficiency, various atom and ring counts, molecular shape, flexibility, complexity, and potential toxicity indicators.[11]

Cell Viability by MTT Assay

Human carcinoma cell line A49 (lung cancer), MCF-7 (Human breast cancer), HT-29 (Human colon cancer), and DU145 (Human prostate cancer) were purchased from the National Centre for Cell Sciences (NCCS) Pune. The work was carried out in the Maratha mandal research centre, Karnataka. The cells were inoculated in 96-well flat-bottom microplates, filled with 200 mL medium per well, and incubated overnight at 37°C with 95% humidity. Cells were exposed to various sample concentrations (100, 50, 25, 12.5, 6.25, and 3.125 µg/mL) for cytotoxic tests. Following this, the cells were incubated for another 48 hours. Then, repeatedly rinse the wells with PBS. Incubate at 37°C for four hours after adding MTT staining solution to each well. Add 100 L of DMSO to each well after 4 hours to dissolve the formazan crystals. Using a microplate reader, record the absorbance at 570 nm.[12]

Microscopic Analysis of Apoptosis Induction

Cancer cells were observed to undergo distinct morphological changes after 48 hours of exposure to IC50 of test sample-8 observed by an inverted microscope. The obtained images were compared to a standard and control for the sample-induced characteristics of apoptosis in the cells, like cell rounding, detachment, floating, shrinkage, and cytoplasmic vacuolation.

Apoptosis Analysis by Flow Cytometry

The HT-29 cells were seeded in a 6-well flat bottom microplate containing coverslips and maintained overnight at 37ºC in a CO_2 incubator. The IC_{50} concentration of sample-8 was treated at 24 hours. Flow cytometry determined apoptosis detection according to the method of wlodkowic, pischel.D and Crowley.[13-15]

Bcl2 Assay

The HT-29 cells were inoculated in a six-well microplate with coverslips and maintained overnight at 37ºC in a CO2 incubator. The IC_{50} concentration of sample-8 was treated after 24 hours. Bcl2 assay was determined by flow cytometry according to the method of Alshabi AM, Miyasgita T.[16,17]

Caspase-3 Assay by Flow Cytometry

The HT-29 cells were seeded in a 6-well flat bottom microplate containing coverslips and maintained overnight at 37ºC in a CO2 incubator. The IC_{50} concentration of sample-8 was treated at 24 hrs. Caspase-3 assay was determined by flow cytometry according to the method of Fan T.[18]

Tunel Assay

The HT-29 cells were inoculated in a 6-well microplate with coverslips and maintained overnight at 37ºC in a CO_2 incubator. The IC_{50} concentration of sample-8 was treated at 24 hours. Tunnel assay was determined by flow cytometry according to the method of kyrylkova.[19]

Cell Cycle Analysis by Flow Cytometry

The HT-29 cells were inoculated in a 24-well flat-bottom microplate with coverslips and incubated overnight at 37°C in a CO_2 incubator. IC_{50} concentration of sample-8 was treated after 12 hours. The cell cycle was analyzed by flow cytometry according to the method of Pozarowski.[20]

Statistical Analysis

Using Microsoft Excel 2013 and Graph Pad Prism Version 5, experimental data processing was performed for statistical analysis. The results were expressed as the mean standard deviation of at least three more independent experiments. The t-test was used to identify statistically significant differences between means when the *p-value* was less than 0.05.

RESULTS

In-silico Studies

A list of eight selected ligands by structure-based drug design approach is depicted in Figure 1. The Scoring profile of ligands with target proteins like Tubulin protein, EGFR, ER, and Anaplastic lymphoma kinase enzyme was tabulated in Table 1. Figure 2 presents a 2D plot visualization of the hydrogen bond interaction between ligand no-8 and various target proteins. The physicochemical properties, toxicity risk assessment of mutagenicity, tumorigenicity, gonadal toxicity, and irritant effect of the eight samples predicted by *in-silico* method were presented in Tables 2 and 3.

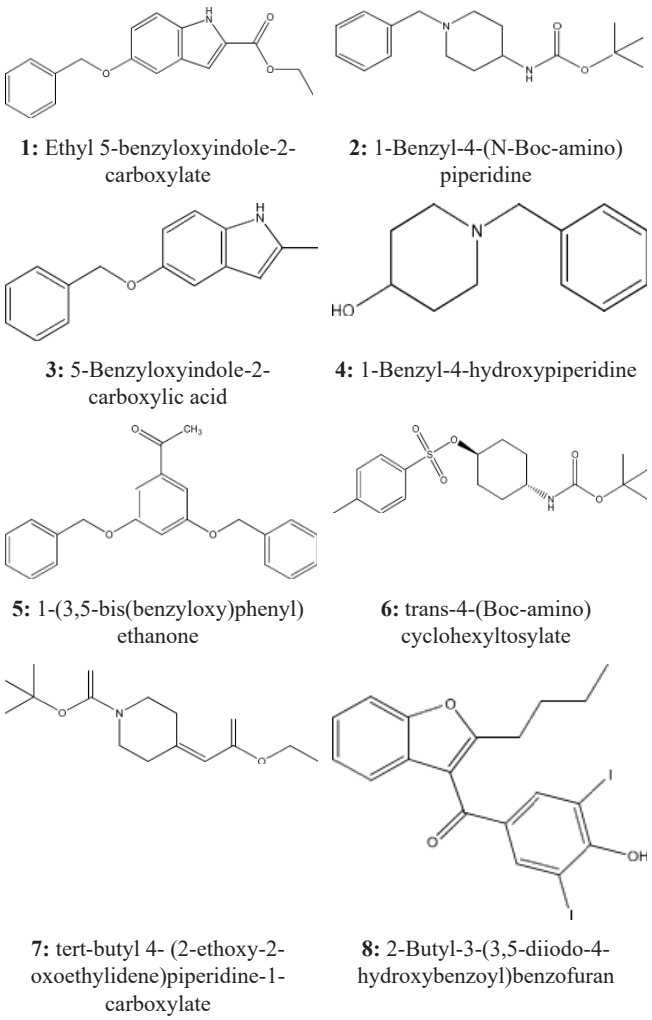

1: Ethyl 5-benzyloxyindole-2-carboxylate

2: 1-Benzyl-4-(N-Boc-amino) piperidine

3: 5-Benzyloxyindole-2-carboxylic acid

4: 1-Benzyl-4-hydroxypiperidine

5: 1-(3,5-bis(benzyloxy)phenyl) ethanone

6: trans-4-(Boc-amino) cyclohexyltosylate

7: tert-butyl 4- (2-ethoxy-2-oxoethylidene)piperidine-1-carboxylate

8: 2-Butyl-3-(3,5-diiodo-4-hydroxybenzoyl)benzofuran

Figure 1: List of selected ligands by structure-based drug design approach.

Table 1: Scoring profile of ligands with target proteins

Ligands	*MVD score*			
	Tubulin (1SA0)	*EGFR (1M17)*	*ER (3ERT)*	*ALK (6MX8)*
N-Deacetyl-N-(2-mercaptoacetyl) colchicine (Co crystalized ligand)	-188.65			
Erlotinib (Co crystalized ligand)		-111.74		
4-hydroxy temoxifen (Co crystalized ligand)			-163.49	
Brigatinib (Co crystalized ligand)				-125.17
1	-112.90	-114.920	-107.28	-113.12
2	-98.311	-88.014	-100.13	-95.13
3	-111.57	-101.570	-109.91	-104.22
4	-113.92	-94.95	-97.59	-89.60
5	-121.30	-108.48	-116.92	-110.91
6	-115.68	-95.61	-118.52	-106.93
7	-100.75	-83.89	-96.18	-93.86
8	-137.24	-120.48	-125.70	-121.920

Table 2: Physicochemical properties of selected ligands anticipated by *in-silico* approach

Ligands	*Physicochemical properties (Lipinski's rule of five)*			
	M. Wt(g/mol)	*ClogP*	*HBA*	*HBD*
1.	295.33	3.420	4	1
2.	290.40	2.923	4	1
3.	267.28	2.586	4	2
4.	191.27	1.563	2	1
5.	332.39	4.22	3	0
6.	369.480	3.277	6	1
7.	269.34	2.592	5	0
8.	546.0	5.49	3	1

Table 3: Assessment of Mutagenicity, Tumorigenicity, Gonadal toxicity, and Irritant effect by *in-silico*

Ligands	*Mutagenicity*	*Tumorigenicity*	*Gonadal toxicity*	*Irritant effect*
1.	No	No	No	No
2.	No	No	No	No
3.	No	No	No	No
4.	No	No	No	No
5.	No	No	No	No
6.	High	No	No	No
7.	No	No	No	No
8.	No	No	No	No

Cytotoxicity by MTT Assay Method

The dose-dependent nature of the growth-inhibiting effect of eight samples on A549, MCF-7, HT-29, and DU145 cancer cells was revealed by MTT assay. The IC_{50} of the eight samples is

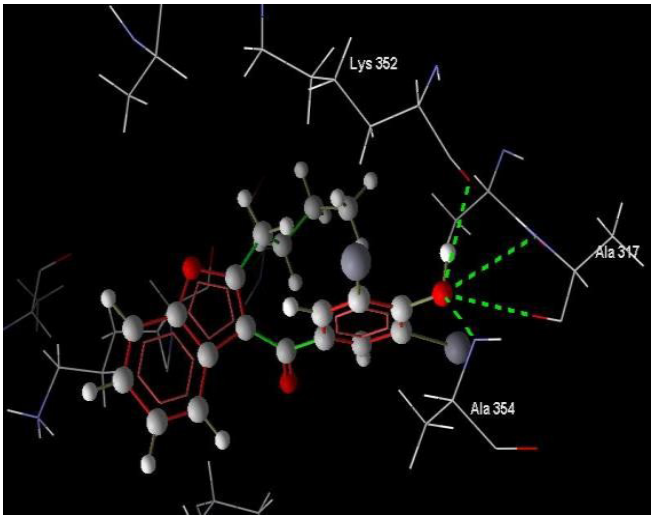

2-Butyl-3-(3,5-diiodo-4-hydroxybenzoyl) benzofuran interact with Tubulin(O18 with Ala354, Ala-317, Ala317 and Lys-352).

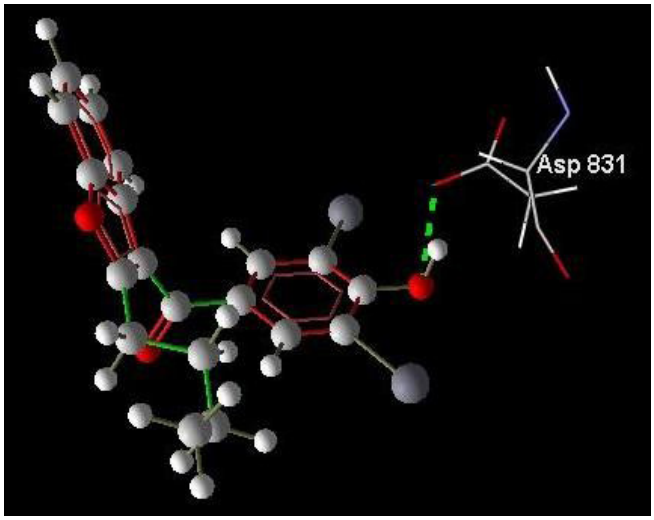

2-Butyl-3-(3,5-diiodo-4-hydroxybenzoyl) benzofuran interact with EGFR (Asp 831)

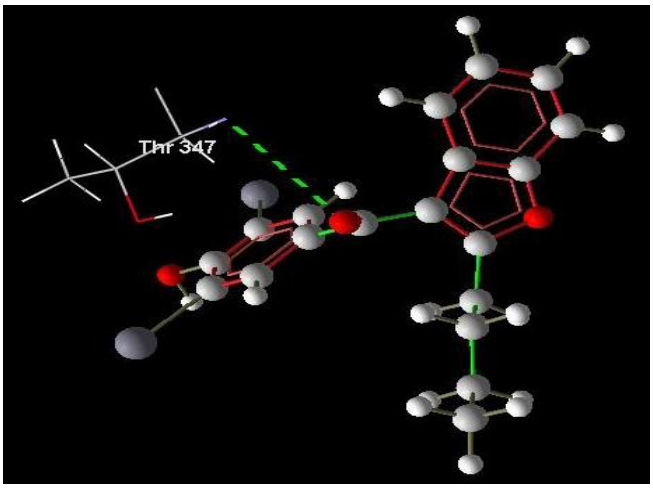

2-Butyl-3-(3,5-diiodo-4-hydroxybenzoyl) benzofuran interact with ER (Thr 347)

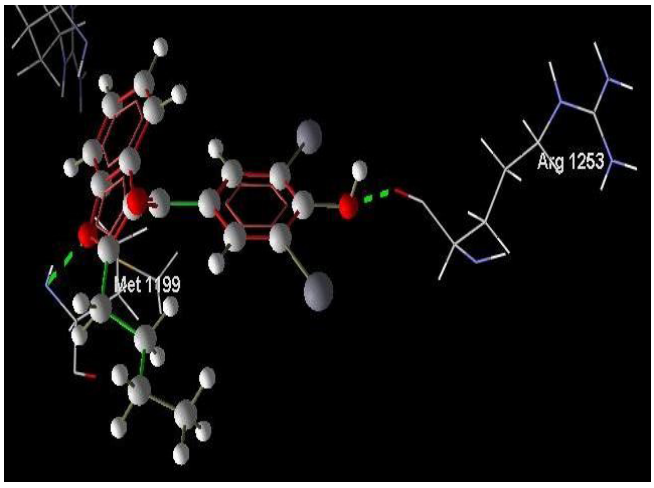

2-Butyl-3-(3,5-diiodo-4-hydroxybenzoyl) benzofuran interact with ALK (O8 Arg-1253, O- in benzofuran ring - Met 1199)

Figure 2: Ligand-protein interaction profile by MVD-2D plot), Hydrogen bonds are mentioned in a discontinuous line green color.

depicted in Figure 3. All eight samples showed cytotoxicity against A549, MCF-7, HT-29 and DU145 cancer cells (Figure 3A-D). Sample 8 showed a higher cytotoxic effect against A549, MCF- 7, HT-29, and DU145 cancer cells (IC_{50}:10.66, 6.05, 5.17, 7.02 µg/mL) compared to the standard doxorubicin effect (IC_{50}:14.54, 5.96, 2.4, 6.3 µg/mL). Sample 8 was found to have a more significant cytotoxic impact than doxorubicin on human lung cancer cells. Sample 7 also demonstrated a significant cytotoxic effect against A549, MCF-7, HT-29, and DU145 cancer cells (IC_{50}: 18.04, 90.14, 42.75, and 26.13 µg/mL) in a level compared to standard doxorubicin (Figure 4). From Figure 5, sample 8 again showed significant toxicity against A549, MCF-7, HT-29, and DU145 cancer cells and exhibited a concentration-dependent decline in viability. However, more potent activity was observed against the A549, MCF-7, compared to the standard doxorubicin. Therefore,

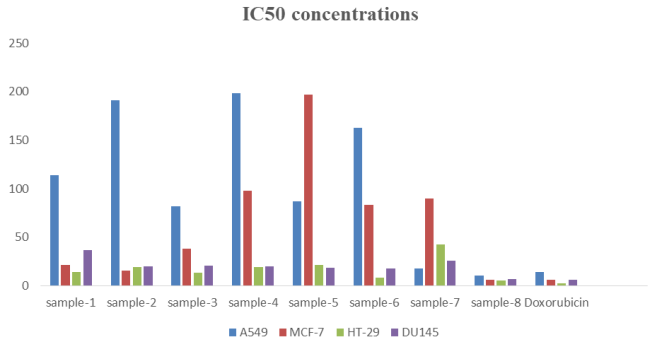

Figure 3: IC^{50} concentrations of test samples by MTT assay.

the cell viability tests demonstrated that sample-8 is a dose-dependently efficacious anti-proliferative agent in proliferating cancer cells.

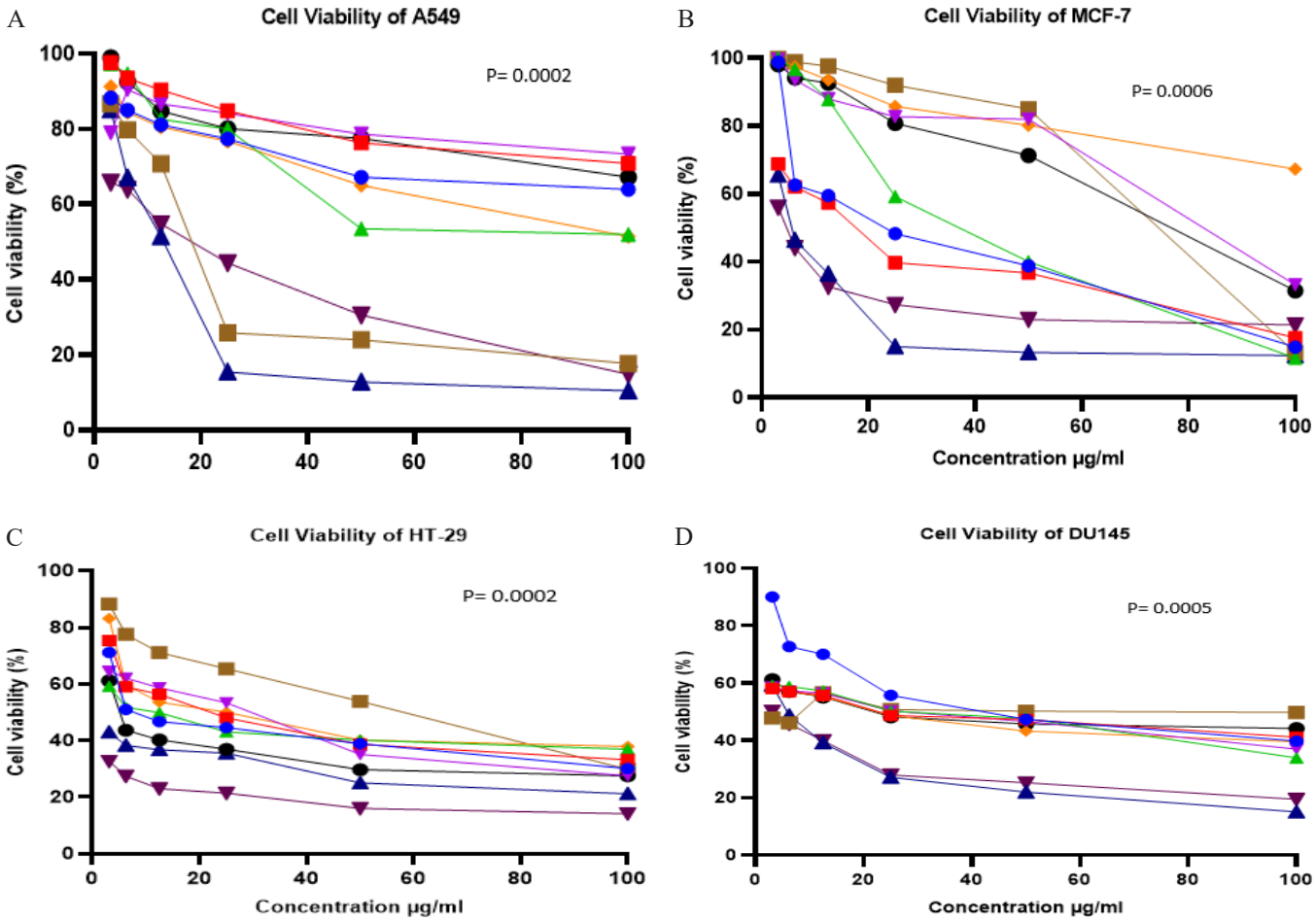

Figure 4: Cancer cells viability by MTT assay A) A549, B) MCF-7, C) HT-29, and D) DU145 at various concentrations (100, 50, 25, 12.5, 6.25, 3.125 µg/ml) of sample

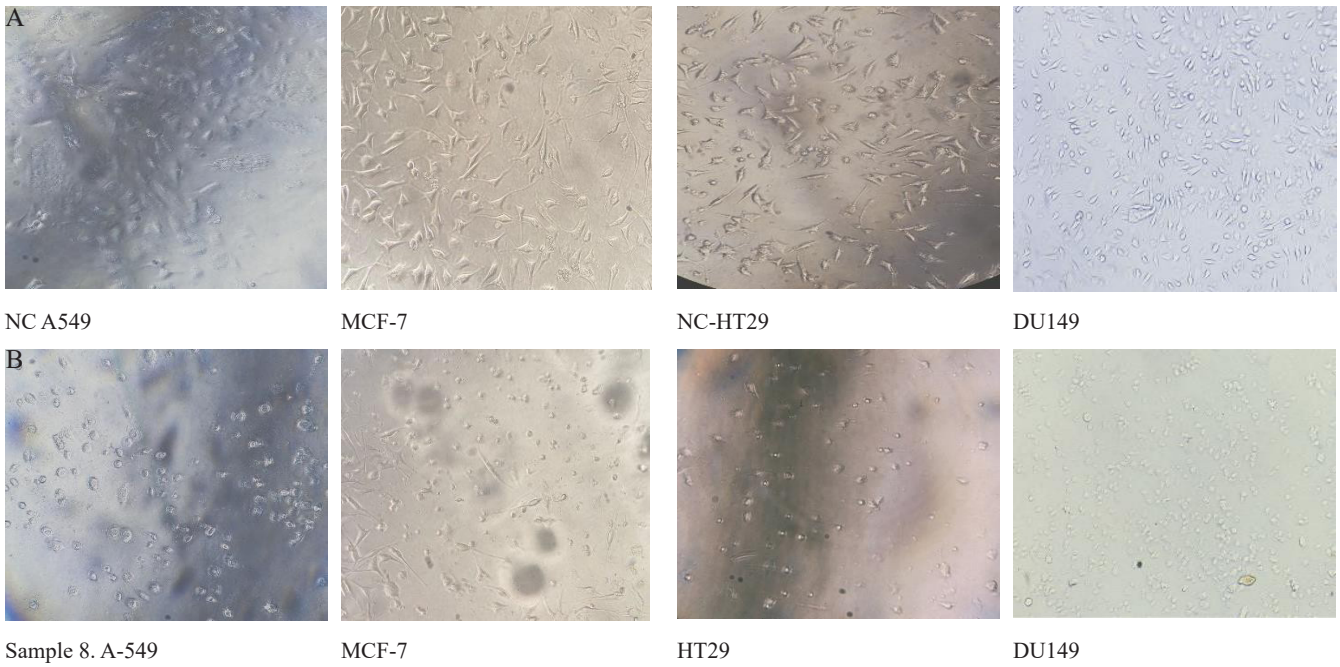

Figure 5: (A) Morphological analysis of NC of the A549, MCF-7, HT-29, and DU145 cancer cells (B) the cells exposed to IC50 of sample 8 for 48 hr.

Table 4: Apoptosis detection assay by flow-cytometry

Sl.NO	*Treatments*	*Early apoptosis*			*Late apoptosis*			*Total Apoptosis*
		1st	*2nd*	*Mean*	*1st*	*2nd*	*Mean*	
1	NC	1.170	1.01	1.090	1.80	1.96	1.88	2.970
2	Apo 8	15.40	15.60	15.50	5.29	5.30	5.29	20.790

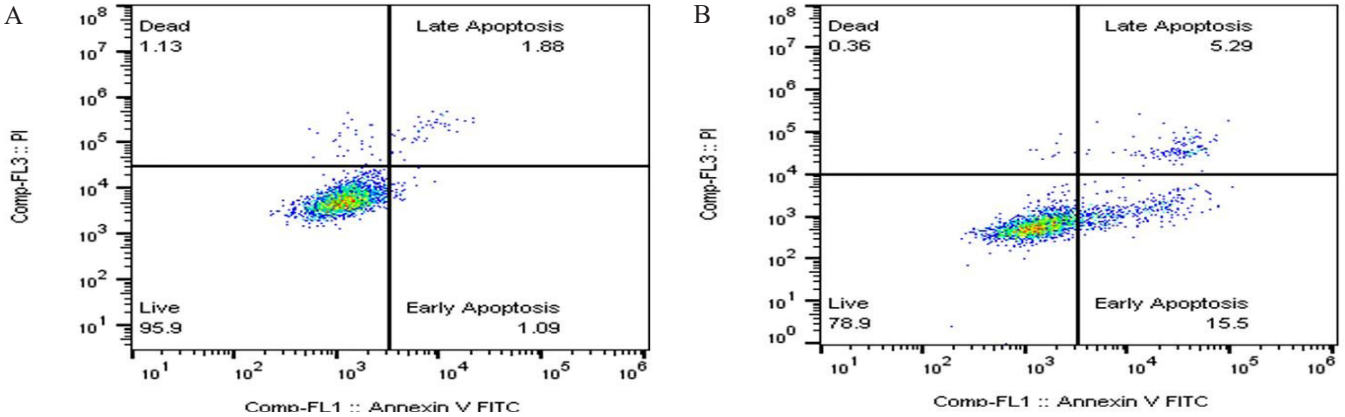

Figure 6: Annexin V apoptosis of control and treated cell analysis. A) Apoptosis-NC B) Apoptosis-sample 8

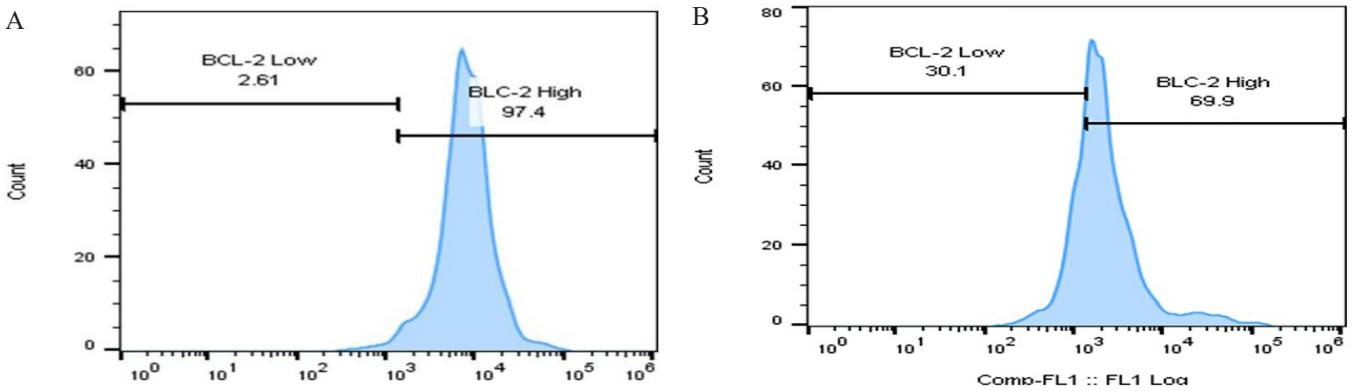

Figure 7: BCL-2 regulated apoptosis of control and treated cell analysis. A) Apoptosis-NC, B) Apoptosis-sample

Microscopic Analysis of Apoptotic Cells

An inverted microscope showed that cancer cells endure distinct morphological changes after 48 hours of exposure to IC_{50} of test sample-8. According to the images acquired, treatment with the test sample caused cell rounding, detachment, floating, shrinkage, and cytoplasmic vacuolation, all signs of apoptosis in the cells, compared to a standard control. (Figure 5A and B).

Apoptosis Detection Assay

The membrane of early apoptotic cells emits green fluorescence. The nucleus's red fluorescence and the cellular membrane's green fluorescence are visible in dead cells. There is little or no fluorescence in living cells. The Annexin V/PI assay can be utilized to identify apoptosis or necrosis. PI (propidium iodide) stains positively on necrotic cells, whereas Annexin V stains positive on apoptotic cells. Annexin V and PI have no staining effect on living cells. Annexin V/PI staining results indicated that sample-8 at the IC50 concentration substantially induces early apoptosis (FITC-Annexin-V+/PI) in HT-29 cells compared to the control (Figure 6). Flow cytometry measurements of average apoptotic cells confirmed the early apoptotic effects of sample 8. Thus, it has been demonstrated that sample 8 induces cancer cells to undergo significant apoptosis (Table 4).

Table 5: Detection of apoptosis of by BCL2- Assay

Sl No.	*Treatments*	*Bcl-2 low (Mean ± SD)*	*Bcl-2 high (Mean ± SD)*
1	NC	2.61 ± 0.04	97.40± 0.280
2	Bcl-2 (sample- 8)	30.40± 0.42	69.90 ± 0.700

BCL2- Assay

In order to confirm whether sample-8 anti-proliferative effect is dependent on Bcl2, the expression of Bcl2 in sample-8 treated cells was examined. Compared with the control, the expression level decreased in HT-29 cells treated with sample-8 for 24 hours at IC_{50} concentration. (Figure 7, Table 5).

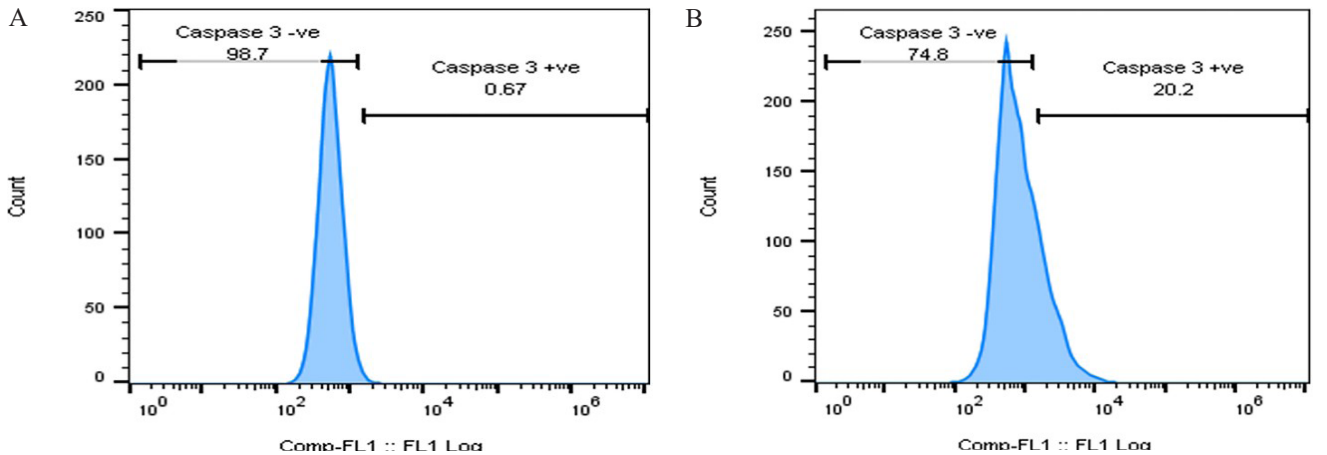

Figure 8: Caspase-3 is regulated apoptosis of control and treated cell analysis A) Apoptosis-NC, B) Images: Apoptosis-sample 8

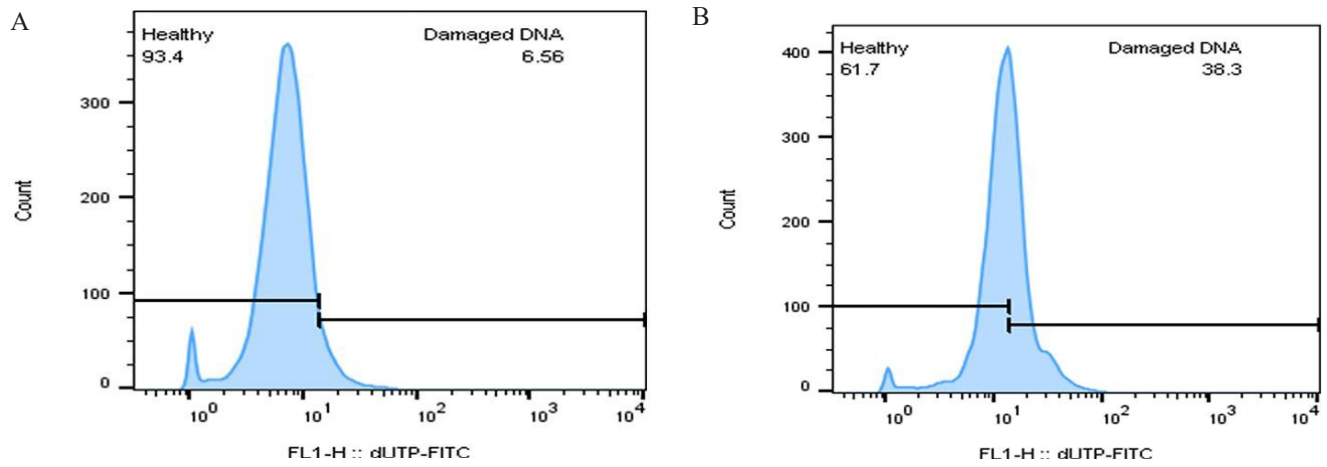

Figure 9: TUNEL-positive cells histograms of control and treated cell analysis A) Apoptosis-NC, B) Images: Apoptosis-sample 8

Table 6: Apoptosis by the activation of Caspase-3

Sl No.	*Treatments*	*Caspase-3 -ve (Mean ± SD)*	*Caspase-3 +ve (Mean ± SD)*
1	NC	98.70 ± 0.2	0.67 ± 0.007
2	Caspase-3 (Sample no-8)	74.8 ± 0.1	20.2 ± 0.1

Table 7: TUNEL assay apoptotic index

Sl No.	*Treatments Mean ± SD*	*Healthy DNA*	*Damaged DNA*
		Mean ± SD	
1	NC	93.80 ± 0.85	5.90 ± 0.92
2	Tunnel Assay (Sample no-8)	61.90 ± 1.30	38.9 ± 0.86

Caspase-3 Activity

The activation of caspase-3, an essential apoptotic pathway executor, was investigated to better understand whether HT-29 cell death was noticed as a result of the stimulation of the apoptotic pathway. Caspase-3 (+ve) was significantly activated by exposure to the IC_{50} concentration of sample 8, which significantly diminished the caspase-3 (-ve) level (Figure 8: Table 6).

TUNEL Analysis

The TUNEL assay results showed that the investigation of the DNA fragmentation caused by treating HT-29 cells with sample-8 IC50 after 24 hours. The results indicated that DNA fragmentation in treated cells was approximately 6.5 times higher than in untreated cells. (Table 7, Figure 9).

Cell Cycle by Flowcytometry

Flow cytometry's analysis of the cell cycle identifies cells at various phases of division by measuring the variation in their DNA content. Figure 10 demonstrates that sample-8 inhibited 50% of HT-29 cells in the G0/G1 phase of the cell cycle at the IC_{50} concentration (Table 8).

Table 8: Cell cycle analysis at different stages

	G1-G0 Phase	*S-Phase*	*G2-M Phase*
Control	84.40	11.60	3.020
	85.20	12.40	2.40
Cellcycle Sample-8	75.10	17.50	6.1
	76.50	16.0	5.1

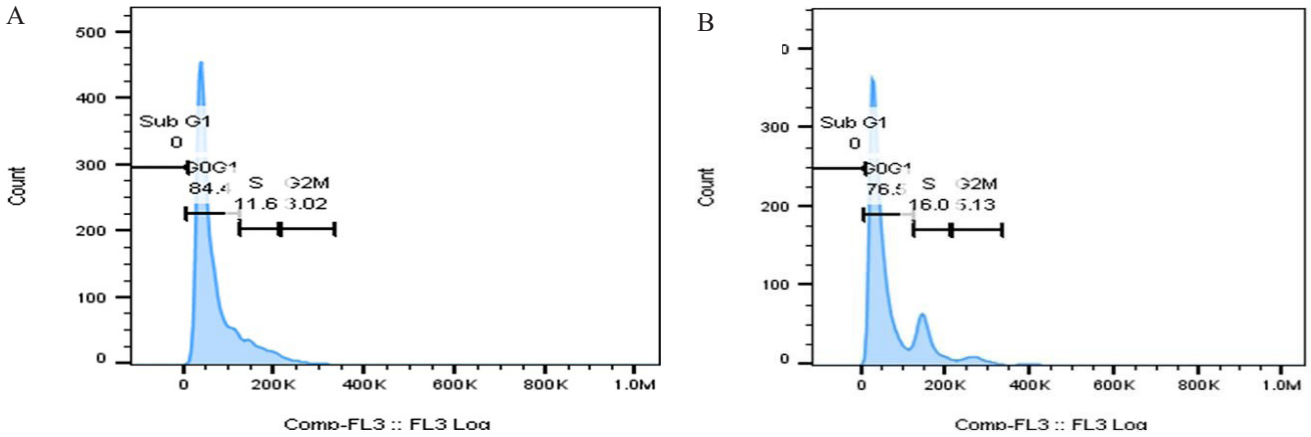

Figure 10: Sequence of cell cycle events of control and treated cell analysis. A. Apoptosis-NC, B) Images: Apoptosis-sample 8

DISCUSSION

Target proteins were chosen based on the pathophysiology of cancer. Methodologies for computer-aided drug design have aided in developing agents for treating cancer that are both highly effective and low toxic. To target tubulin dynamics, researchers are developing new chemotherapeutic agents. The binding site of colchicine is an essential pocket for potential destabilizers of tubulin polymerization. Colchicine binds tightly to unpolymerized –β-tubulin and creates a tubulin-colchicine complex that results in a curved tubulin dimer, thereby preventing the tubulin from adopting a straight structure. This is due to a steric confrontation between colchicine and tubulin, which inhibits microtubule assembly and effects microtubule and cytoskeleton function. Microtubule elongation is avoided by the tubulin-colchicine complex's attachment to the terminals of microtubule polymers.[21,22]

The epidermal growth factor receptor (EGFR), an affiliate of the ErbB family of receptor tyrosine kinases (RTKs), is essential to the physiology of epithelial cells. EGFR's physiological function is to regulate the growth and homeostasis of epithelial tissue. The EGFR is a promoter of tumorigenesis in pathological contexts, particularly lung and breast cancer as well as glioblastoma. It is frequently mutated and overexpressed in diverse varieties of human cancer, and it is the target of multiple clinically employed cancer therapies.[23]

Oestrogen, a female reproductive hormone, exerts its physiological effects primarily via the estrogen receptor subtypes ERα- andβ. Estrogen receptor alpha is crucial in the mammary gland and the uterus. Uncontrolled cellular proliferation results from the deregulation of the numerous coregulators, including alterations in their concentrations or genetic dysfunction. Since the estrogen receptor is responsible for breast cancer initiation and progression, it is one of the chemotherapy's target proteins.[24, 25]

Anaplastic lymphoma kinase (ALK), also known as ALK tyrosine kinase receptor or CD246 (cluster of differentiation 246), is an enzyme involved in cell growth that is encoded by the ALK gene in humans. The ALK gene can cause cancer in three ways: by forming a fusion gene with another gene, by acquiring additional copies of the gene, and by mutations in its DNA code. Mutant forms of ALK are present in numerous malignancies, including neuroblastoma, non-small cell lung cancer, and anaplastic large cell lymphoma. As a consequence of these modifications, cancer cells may grow more rapidly. The detection of alterations in the ALK gene in tumour tissue may enhance cancer treatments.[26, 27] Based on the aforementioned fact, designed compounds were included in the present *in-silico* analysis to evaluate their inhibitory effect on the Tubulin (1SA0), EGFR (1M17), ER (3ERT), and ALK enzyme (6MX8) using molecular docking studies with the Molegro virtual docker. We opted for eight molecules (Figure-1) with a high docking score from among the eighty-six molecules.

Pfizer's rule of five/Lipinski's rule five/ rule of five (RO5) is a rule of thumb used to determine whether a chemical compound exhibiting specific pharmacological or biological properties would make a likely orally active medication. Christopher In 1997, A. Lipinski proposed the rule based on the observation that most drugs taken orally are moderately lipophilic molecules of relatively small dimensions.[29] In the human body, there is a rule describing how molecular drug properties affect pharmacokinetics. However, it does not determine whether a compound is pharmacologically active. To ensure drug-like properties are maintained during the drug discovery process, Lipinski's rule should be kept in mind when optimizing a pharmacologically active lead structure step-by-step.[29] Drugs compliant with the RO5 tend to have lower attrition rates during clinical trials, increasing their chances of reaching the market.[28,30] Lipinski's rule of five states that accessibility of the orally administered drugs to their site of action depends on their physicochemical properties. We evaluated physicochemical properties (Table 2) like the molecular weight is less than 350 Unified mass, the computed partition coefficient is 1.5-5.5, the hydrogen bond donor is 1–2, and hydrogen bond acceptor is 3–6. All selected molecules obey Lipinski's rule of five.

An alert for toxicity risk indicates the structure is potentially harmful in relation to the risk category. The major toxicity risk, like Irritating effects, reproductive effects, Mutagenicity and tumorigenicity, was assessed by employing the DataWarrior v04.04.04. The toxicity potential was graded

as high risk, medium risk and low risk. Selected ligands are free from major toxicity risks (Table 3), but ligand 6 may have only Mutagenicity.

Apoptosis and the cell cycle were analysed to investigate the pharmacological effects of sample 8 on HT-29 cells. Treatment with sample 8 increased the apoptosis rate of HT-29 cells, with 80% of cells in the early stage of apoptosis at the IC50 concentration of 5µg/mL. However, sample-8 inhibited the cells in the G0/G1 phase of the cell cycle, with 50% of the cells in the G0/G1 phase of the cell cycle at 5 µg /mL of sample-8, and the fraction of arrested cells increased with increasing concentrations of fucoidan. Moreover, the migration of HT-29 cells tended to decrease as sample-8 concentration and incubation time increased. These results suggested that sample-8 had a greater impact on cell cycle and apoptosis.

Annexin V- (FITC) was used to examine the inhibitory mode caused by the IC50 concentration of sample 8 in HT-29 (Human Colon Cancer) cells. Apoptosis was confirmed by Annexin V- (FITC) in the treated cells, which is in accordance with the morphological changes observed under the microscope.[31,32] The annexin apoptosis process eliminates damaged, senescent, or unwanted cells from tissues. The outer surface of a normal cell membrane contains uncharged phospholipids (PS), and the inner surface contains negative phospholipids (NP). During apoptosis, negatively charged PS moves from the inner leaflet of a cell's plasma membrane to the outer leaflet, where it is exposed to the exterior environment. Annexin V, a human anticoagulant, is a Ca+2 dependent phospholipid-binding protein of 35-36 kDa with a high affinity for PS. A biotin- or fluorophore-labeled annexin V can be used to identify apoptotic cells. The fluorescent nucleus dye, propidium iodide (PI), stains dead cells crimson by binding tightly to their nucleic acids. It is impermeable to both living and apoptotic cells.[33,34]

When analyzing the apoptosis-inducing properties of sample-8, the treated cells exhibited significant DNA fragmentation. Apoptotic morphological changes and DNA fragmentation result from the activation of caspases via selective cleavage of vital cellular substrates. The detection of caspase-3 activity in treated cells and spheroids demonstrated that sample-8 activates caspase-3. Enzymes such as DNase are triggered due to caspase-3 activation, resulting in DNA fragmentation and apoptosis. Increased expression levels of Bax and cleaved caspase-3 were observed. Consequently, sample-8 induces apoptosis by modulating the Bax/Bcl-2 ratio and increasing the level of cleaved caspase-3, thereby triggering the intrinsic and possibly extrinsic apoptosis pathway with promoting downstream signaling pathways to the death. These studies may elucidate the inevitable relationship between the cell cycle and apoptosis and the mechanism by which 2-Butyl-3-(3, 5-diiodo-4-hydroxy benzoyl) benzofuran induces the death of HT-29 cells.

CONCLUSION

Based on the findings, 2-Butyl-3- (3, 5-diiodo-4-hydroxy benzoyl) benzofuran was found to have potent cytotoxic efficacy towards A49, MCF-7, HT-29, and DU145 cancer cells. Sample 8 showed equipotent activity against colorectal cancer cells and more potent against Human lung cancer, compared to doxorubicin. The proposed mechanism of action may be caspase-3 activation. As a consequence of caspase-3 activation, enzymes such as DNase are activated, leading to DNA fragmentation and apoptosis, and DNA fragmentation was 6.5 times greater than in untreated cells. The IC50 concentration of Sample 8 inhibited 50% of HT-29 cells during G0/G1 phase. In the present investigation, we evaluated the potential anticancer properties of sample-8 on colorectal cancer (HT-29) cells. Future research should focus on the effect on human lung cancer cells.

REFERENCES

1. Cancer [Internet]. World Health Organization. World Health Organization; 2022 [cited 2023Apr4]. Available from: https://www.who.int/news-room/fact-sheets/detail/cancer.
2. Sak ZHA, Süzergöz F, Kasumov VT, Gürol AO. Anticancer Properties of Fluorinated Aminophenylhydrazines on A549 Lung Carcinoma Cell Line. Iran J Public Health. 2021; 50: 550-60.
3. Khorsandi L, Orazizadeh M, Niazvand F, Abbaspour MR, Mansouri E, Khodadadi A. Quercetin induces apoptosis and necroptosis in MCF-7 breast cancer cells. Bratislava Medical Journal. 2017;118(02):123–8.
4. Wagner EK, Nath N, Flemming R, Feltenberger JB, Denu JM. Identification and characterization of small molecule inhibitors of a plant homeodomain finger. Biochemistry. 2012;51(41):8293– 306.
5. Carlsson B, Singh BN, Temciuc M, Nilsson S, Li Y-L, Mellin C, et al. Synthesis and preliminary characterization of a novel antiarrhythmic compound (KB130015) with an improved toxicity profile compared with amiodarone. Journal of Medicinal Chemistry. 2002;45(3):623–30.
6. De Sousa NF, Scotti L, de Moura ÉP, dos Santos Maia M, Rodrigues GC, de Medeiros HI, et al. Computer aided drug design methodologies with natural products in the drug research against alzheimer's disease. Current Neuropharmacology. 2022;20(5):857–85.
7. Pubchem Structure Search [Internet]. National Center for Biotechnology Information. PubChem Compound Database. US National Library of Medicine; [cited 2023Apr4]. Available from: https://pubchem.ncbi.nlm.nih.gov/search/search.cgi
8. DrugBank release version 5.1.10 [Internet]. DrugBank Release Version 5.1.10 | DrugBank Online. [cited 2023Apr4]. Available from: https://www.drugbank.ca/releases/latest
9. Swissadme [Internet]. SwissADME. [cited 2023Apr4]. Available from: http://www.swissadme.ch/index.php.
10. Xiong G, Wu Z, Yi J, Fu L, Yang Z, Hsieh C, et al. ADMETlab 2.0: An integrated online platform for accurate and comprehensive predictions of ADMET properties. Nucleic Acids Research. 2021;49(W1).
11. Sander T, Freyss J, von Korff M, Rufener C. Datawarrior: An open-source program for Chemistry Aware Data Visualization and analysis. Journal of Chemical Information and Modeling. 2015;55(2):460–73.
12. Wadhwa R, Paudel KR, Chin LH, Hon CM, Madheswaran T, Gupta G, Panneerselvam J, Lakshmi T, Singh SK, Gulati M, Dureja H. Anti-inflammatory and anticancer activities of Naringenin-loaded liquid crystalline nanoparticles in-vitro. Journal of food biochemistry. 2021 Jan;45(1):e13572.

13. Wlodkowic D, Skommer J, Darzynkiewicz Z. Flow cytometry-based apoptosis detection. Methods in Molecular Biology. 2009;:19–32.
14. Pischel D, Buchbinder JH, Sundmacher K, Lavrik IN, Flassig RJ. A guide to automated apoptosis detection: How to make sense of imaging flow cytometry data. PLOS ONE. 2018;13(5).
15. Crowley LC, Marfell BJ, Scott AP, Waterhouse NJ. Quantitation of apoptosis and necrosis by annexin V binding, propidium iodide uptake, and flow cytometry. Cold Spring Harbor Protocols. 2016;2016(11).
16. Alshabi AM, Alkahtani SA, Shaikh IA, Orabi MAA, Abdel-Wahab BA, Walbi IA, et al. Phytochemicals from Corchorus Olitorius methanolic extract induce apoptotic cell death via activation of caspase-3, anti-bcl-2 activity, and DNA degradation in breast and lung cancer cell lines. Journal of King Saud University - Science. 2022;34(7):102238.
17. Miyashita T, Krajewski S, Krajewska M, Wang HG, Lin HK, Liebermann DA, Hoffman B, Reed JC. Tumor suppressor p53 is a regulator of bcl-2 and bax gene expression in-vitro and in vivo. Oncogene. 1994; 9(6):1799–805.
18. Fan T-J, Han L-H, Cong R-S, Liang J. Caspase family proteases and apoptosis. Acta Biochimica et Biophysica Sinica. 2005;37(11):719–27.
19. Kyrylkova K, Kyryachenko S, Leid M, Kioussi C. Detection of apoptosis by TUNEL assay. Methods in Molecular Biology. 2012;:41–7.
20. Pozarowski P, Darzynkiewicz Z. Analysis of cell cycle by flow cytometry. Checkpoint Controls and Cancer: Volume 2: Activation and Regulation Protocols. 2004:301-11.
21. Schulze-Osthoff K, Walczak H, Dröge W, Krammer PH. Cell nucleus and DNA fragmentation are not required for apoptosis. Journal of Cell Biology. 1994;127(1):15–20.
22. Ravelli RBG, Gigant B, Curmi PA, Jourdain I, Lachkar S, Sobel A, et al. Insight into tubulin regulation from a complex with colchicine and a stathmin-like domain. Nature. 2004;428(6979):198–202.
23. Lu Y, Chen J, Xiao M, Li W, Miller DD. An overview of tubulin inhibitors that interact with the colchicine binding site. Pharmaceutical Research. 2012;29(11):2943–71.
24. Sigismund S, Avanzato D, Lanzetti L. Emerging functions of theegfrin cancer. Molecular Oncology. 2017;12(1):3–20.
25. Saha Roy S, Vadlamudi RK. Role of estrogen receptor signaling in breast cancer metastasis. International Journal of Breast Cancer. 2012;2012:1–8.
26. Ali S, Mondal N, Choudhry H, Rasool M, Pushparaj PN, Khan MA, et al. Current management strategies in breast cancer by targeting key altered molecular players. Frontiers in Oncology. 2016;6.
27. Hallberg B, Palmer RH. Mechanistic insight into ALK receptor tyrosine kinase in human cancer biology. Nature Reviews Cancer. 2013;13(10):685–700.
28. Lipinski CA. Lead-and drug-like compounds: the rule-of-five revolution. Drug discovery today: Technologies. 2004 Dec 1;1(4):337-41. 30.
29. Palmer RH, Vernersson E, Grabbe C, Hallberg B. Anaplastic lymphoma kinase: Signalling in development and disease. Biochemical Journal. 2009;420(3):345–61. 29.
30. Oprea TI, Davis AM, Teague SJ, Leeson PD. Is there a difference between leads and drugs? A historical perspective. Journal of chemical information and computer sciences. 2001 Sep 24;41(5):1308-15.
31. Leeson PD, Springthorpe B. The influence of drug-like concepts on decision-making in medicinal chemistry. Nature reviews Drug discovery. 2007 Nov;6(11):881-90.
32. Yeh SH-H, Kong F-L, Lin M-H. Visualization of apoptosis: Annexin V Imaging. Personalized Pathway-Activated Systems Imaging in Oncology. 2017;:233–43.
33. Duensing TD, Watson SR. Assessment of apoptosis (programmed cell death) by flow cytometry. Cold Spring Harbor Protocols. 2018;2018(1).
34. Lizard G, Fournel S, Genestier L, Dhedin N, Chaput C, Flacher M, Mutin M, Panaye G, Revillard JP. Kinetics of plasma membrane and mitochondrial alterations in cells undergoing apoptosis. Cytometry: The Journal of the International Society for Analytical Cytology. 1995 Nov 1; 21(3):275-83.